



**CISTER**

Research Center in  
Real-Time & Embedded  
Computing Systems

# Technical Report

---

## **On Packet Size and Error Correction Optimisations in Low-Power Wireless Networks**

**Claro Noda**

**Shashi Prabh**

**Mário Alves**

**Thiemo Voigt**

---

CISTER-TR-131001

Version:

Date: 10-08-2013

# On Packet Size and Error Correction Optimisations in Low-Power Wireless Networks

Claro Noda, Shashi Prabh, Mário Alves, Thiemo Voigt

CISTER Research Unit

Polytechnic Institute of Porto (ISEP-IPP)

Rua Dr. António Bernardino de Almeida, 431

4200-072 Porto

Portugal

Tel.: +351.22.8340509, Fax: +351.22.8340509

E-mail:

<http://www.cister.isep.ipp.pt>

## Abstract

In wireless networks that operate in those bands where spectrum sharing occurs across a variety of wireless technologies, such as the license-free Industrial Scientific and Medical (ISM) bands, mitigating interference becomes challenging. Addressing interference is an important aspect for the design and development of solutions intended to satisfy the demands of applications requiring QoS guarantees. In this paper, we investigate dynamic radio resource adaptation techniques based on instantaneous spectrum usage. Using a novel metric to quantify the spectrum usage, we address packet size and error correction code overhead optimisations. On one hand, large payloads lead to energy and throughput gains due to the amortisation of the transmission overheads, but on the other hand, larger payloads imply larger resource wastage in the event of packet collisions. Using real-world data, we found that payload size in the neighbourhood of 100 bytes leads to near-optimal performance in general in the IEEE 802.15.4 networks. Our data also shows that for very high interference scenarios, erasure codes capable of correcting 10% of the packet payload can provide an equivalent Signal to Interference plus Noise Ratio (SINR) gain of 25 dB with probability greater than 0.6. This is significant for interference management and for increasing spatial re-use by employing lower transmission power. We show that erasure codes drastically improve energy-efficiency and throughput of low-power wireless links. In the heavy interference regime, even though interference doubles the energy-per-usable-bit cost, erasure codes remain cost-effective for very large payload sizes, up to 1500 bytes. Finally, we discuss interference-dependent dynamic adjustment of the correction capacity of erasure codes.

# On Packet Size and Error Correction Optimisations in Low-Power Wireless Networks

Claro Noda, Shashi Prabh, and Mário Alves  
CISTER/INESC-TEC, ISEP, Politécnico do Porto, Portugal  
{cand, ksp, mjf}@isep.ipp.pt

Thiemo Voigt  
SICS and Uppsala University, Sweden  
thiemo@sics.se

**Abstract**—In wireless networks that operate in those bands where spectrum sharing occurs across a variety of wireless technologies, such as the license-free Industrial Scientific and Medical (ISM) bands, mitigating interference becomes challenging. Addressing interference is an important aspect for the design and development of solutions intended to satisfy the demands of applications requiring QoS guarantees. In this paper, we investigate dynamic radio resource adaptation techniques based on instantaneous spectrum usage. Using a novel metric to quantify the spectrum usage, we address packet size and error correction code overhead optimisations. On one hand, large payloads lead to energy and throughput gains due to the amortisation of the transmission overheads, but on the other hand, larger payloads imply larger resource wastage in the event of packet collisions. Using real-world data, we found that payload size in the neighbourhood of 100 bytes leads to near-optimal performance in general in the IEEE 802.15.4 networks. Our data also shows that for very high interference scenarios, erasure codes capable of correcting 10% of the packet payload can provide an equivalent Signal to Interference plus Noise Ratio (SINR) gain of 25 dB with probability greater than 0.6. This is significant for interference management and for increasing spatial re-use by employing lower transmission power. We show that erasure codes drastically improve energy-efficiency and throughput of low-power wireless links. In the heavy interference regime, even though interference doubles the energy-per-usable-bit cost, erasure codes remain cost-effective for very large payload sizes, up-to 1500 bytes. Finally, we discuss interference-dependent dynamic adjustment of the correction capacity of erasure codes.

**Index Terms**—Wireless Channel Quality, ISM Bands, Interference, Dynamic Resource Adaptation, Forward Error Correction, Low-Power Wireless Networks

## I. INTRODUCTION

The deployment of co-located wireless networks operating in the same band, such as, the license-free Industrial Scientific and Medical (ISM) bands, is increasingly unavoidable as wireless networks become more and more ubiquitous. These networks usually serve different purposes, use different technologies and are not always designed to communicate with each other. However, since they operate in the same band, they also suffer from performance degradation due to interference.

Some wireless networks, like sensor networks, require low-power operation. In such networks, the Physical (PHY) and Medium Access Control (MAC) layers are typically based on the IEEE 802.15.4 standard, a standard developed for wireless

low-power personal area networks (WPANs). Although sensor network protocols are designed for energy-efficiency, most of them, however, do not explicitly account for interference. Especially in the case of high sustained interference, the overall energy consumption in communications increases due to factors such as excessive retransmissions and decreased sleep times [1].

Low-power wireless networks have led to a flurry of research and standardization processes in the last decade, with reliability and energy efficiency as the primary concerns. On the other hand, the proliferation of the IEEE 802.11 based Wi-Fi networks has been significant, particularly in dense residential areas and office buildings. This trend will further continue with the deployment of the fourth generation mobile cellular networks (LTE/4G). In order to satisfy the increasing data traffic demands, it is not uncommon for network operators to divert load to the unlicensed spectrum, avoiding spectrum licensing costs as well.

Interference in low-power wireless networks has two distinct origins. First, there is the interference that may be experienced by the cumulative effect of concurrent transmissions of nodes, which is well captured by the Signal to Interference plus Noise Ratio (SINR) model. Second, the interference produced by other networks like those based on the IEEE 802.11, operating on overlapping channels have large RF power and spectrum footprint. Such interference from coexisting networks in ISM Bands is typically referred as Cross Technology Interference (CTI).

Addressing CTI to satisfy the Quality of Service (QoS) requirements in low-power wireless networks remains a challenge. In this paper, we explore how low-power communication protocols can benefit by dynamically adapting radio resources, based on the channel condition as quantified by a Channel Quality (CQ) metric, which we define in Section §II. Our experiments show that the packet size and erasure code optimizations provide greater energy efficiency and reliability than fragmentation and reassembly of 6LoWPAN packets. Erasure codes provide significant SINR gain margin which allows a receiver to effectively decode packets transmitted at lower power levels, well under the threshold imposed by interfering signals from the IEEE 802.11 networks (when no erasure

code is used). This “equivalent SINR gain” favours spatial re-usability of the frequency and/or time slots within the low-power wireless network and increases the *practical* margin for adjustments of the transmission power.

Recent sensor network platforms with greater computation capacity provide powerful computing capabilities while maintaining low energy consumption akin to older (low-end) platforms [2], [3]. These resource-rich platforms have increased processing capabilities which make erasure code handling viable and efficient [3]. Moreover, improved radio designs [4] facilitate better spectrum sensing as well as provide hardware support for fast packet framing and assembly.

We make the following contributions in this paper:

- We provide experimental evidence that enlarging the payload of the IEEE 802.15.4 packets up to 500 bytes leads to higher energy-efficiency and higher throughput under moderate or low CTI. This finding is significant for communications among heterogeneous networks, for example, sending IPv6 packets over IEEE 802.15.4 PANs that are currently addressed in the 6LoWPAN standard.
- We provide experimental evidence that erasure codes capable of correcting 10% of the packet payload can provide an equivalent SINR gain of 25 dB with probability greater than 0.6 under heavy CTI conditions. The same erasure code increases the optimal payload sizes and boosts throughput up-to five times for a wide range of channel conditions. Furthermore, using erasure codes reduces the uncertainty in the energy cost of packet transmissions, which simplifies dynamic packet size adaptations.
- We propose a systematic approach for implementing dynamic radio resource adaptation based on wireless channel quality.

The rest of this paper is organized as follows. Section §II describes the metrics and the experimental data used in the paper. Section §III presents experimental results and discusses interference dependent packet size optimizations. Section §IV deals with erasure code usage and code-rate optimizations. We discuss related work in Section §V and conclude the paper with Section §VI.

## II. PRELIMINARIES

In the absence of interference, the Bit Error Rate (BER) at the Physical (PHY) layer is primarily determined by the Signal to Noise Ratio (SNR), the channel condition and the modulation scheme employed. If the bit errors are i.i.d., the Packet Error Rate (PER) can be expressed as a function of the BER and the size of the packet, namely  $PER = 1 - (1 - BER)^l$ , where  $l$  represents the number of bits in the packet. Yet, this PER value can be reduced with spread spectrum techniques [5].

We compute the SNR required to maintain  $PER = 10^{-2}$ , under *Additive White Gaussian Noise* (AWGN) and *Rayleigh* fading channel models, for three packet sizes. Table I shows the results. The largest packets require additional gains of 0.9 and

2.0 dB, respectively. Note that such link margins are attained by increasing the transmission power but without changing the total chip power significantly. We chose  $PER = 10^{-2}$  because this value is sufficiently small to neglect packet losses due to noise and fading. In the following, we present a simple model based on Packet Reception Rate (PRR, defined as  $1 - PER$ ) statistics to estimate energy-per-useful-bit and link throughput. Our model accounts for packet losses due to collisions in a point-to-point link, where transmitters do not use any contention resolution.

### A. Channel Quality (CQ) Metric

Let  $P$  be channel energy sampling period and let  $E_{THR}$  be the energy threshold below which we define the channel to be idle. In our experiments, we chose  $E_{THR}$  to be the energy level required for correct decoding of packets specified by the SINR model. Let  $m_j$  denote the number of  $j$  consecutive samples where the channel was idle, which we call *channel vacancies*. For example, in a sample “100001001001” where 0 indicates idle channel state and 1 indicates measured energy to be larger than the threshold,  $m_2 = 2$ ,  $m_3 = 0$ , and  $m_4 = 1$ . We quantify the wireless channel quality with the CQ metric [6], defined as:

$$CQ(\tau) = \frac{1}{(n-1)^{(1+\beta)}} \sum_{j|(j-1)P > \tau} j^{(1+\beta)} m_j, \quad (1)$$

where  $n$  denotes the total number of channel energy samples and  $\beta > 0$  is a bias parameter that gives (polynomially) larger weights to longer channel vacancies, and  $\tau > 2P$  is the time-scale of interest, which can be the duration of packet transmission. Notice that  $j$  consecutive channel vacancies imply that the channel was idle for at least  $(j-1)P$  time units. CQ takes values in the range  $[0, 1]$ , where larger values indicate better channel quality. Moreover, as discussed below, this metric exhibits strong correlation with PRR. But CQ differs from PRR in that it only accounts for interference and does not consider packet transmissions. Because CQ relies on the receiver channel energy detection, it scales well with node density and channel usage.

On channel energy traces collected by a sensor network deployed in a library building [7], CQ exhibits a strong correlation with PRR shown in Figure 1. In this figure, for the same channel quality, the PRR is higher for the shorter ACK frames than for 100-byte data frames until interference gets very high. Observe that lower energy thresholds,  $E_{THR}$ , tend to produce lower CQ values and vice versa. Further details can be found in [6].

Payload Size	127 B	512 B	1260 B
SNR (dB) <i>AWGN</i>	1.1	1.7	2.0
SNR (dB) <i>Rayleigh</i>	5.9	7.1	7.9

TABLE I: Longer packets require larger SNR to maintain  $PER = 10^{-2}$ . Theoretical SNR values are computed for *AWGN* and *Rayleigh* fading channel models, using the IEEE 802.15.4 PHY parameters except the maximum packet size.

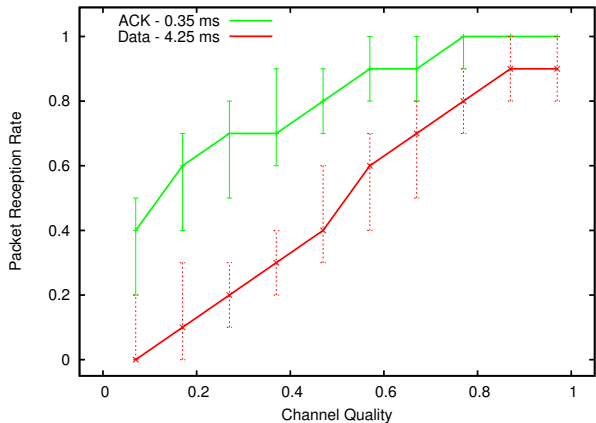


Fig. 1: Correlation of channel quality indicated by  $CQ$  with PRR. Vertical bars represent the inter-quartile range (IQR).

### B. Utility Metrics

The energy-per-useful-bit [8] is a key metric for low-power radios and our objective is to minimize it. Although sensor networks typically operate at relatively low data rates, throughput is often an issue. This issue arises, for example, in order to provide QoS to bursty traffic. Even with very low data rates, the throughput requirement for convergecasts in the neighborhood of a sink node tends to remain high. Interference affects throughput adversely, and its impact on end-to-end performance metrics usually increases with increasing hop-count.

We now define total energy-per-useful-bit and throughput, adapted from the literature. Let  $E_p$  denote the minimum total energy required to transfer a packet over the channel,  $PL$  denote the size of the packet's payload and  $L_p$  denote the latency of packets, which accounts for packet transmission time plus the inter-packet interval (IPI).

*Definition 1.* Energy-per-useful-bit:

$$E_{bit} = \frac{E_p}{PL \cdot PRR}. \quad (2)$$

*Definition 2.* Packet throughput:

$$U_{put} = \frac{PL \cdot PRR}{L_p}. \quad (3)$$

Our total energy-per-useful-bit differs from that in [8] in that we refer to useful bits as those in the data payload, excluding the ones in protocol headers, in order to capture the protocol overhead as well. We estimated  $E_p$  based on 80 mW target power, which includes chip power for both receiver and transmitter modules [9].

### C. Measurement Data

In this study, we base our analysis on channel energy measurements collected by a sensor network deployed in a library building [7]. The sensor network passively monitored all sixteen IEEE 802.15.4 channels, with a sampling period of 23

$\mu$ s. These traces contain continuous sampling segments of 130 ms, spaced by intervals of around 8 s. The major (and perhaps the only) users of the channels were several IEEE 802.11 based Wi-Fi networks under normal operation. Over 500 MAC addresses were registered in two measuring campaigns which were carried out on two different days, with a duration of 3 and 4 hours, respectively. Detailed description of the traces as well as code for all experiments in this paper are available online [7].

The duration of packets in IEEE 802.15.4 based sensor networks is  $512 - 4256 \mu$ s and they can accommodate a maximum payload of 127 octets [10]; the corresponding duration in the IEEE 802.11 based networks is  $202 - 1,906 \mu$ s and  $194 - 542 \mu$ s for the versions IEEE 802.11b and IEEE 802.11g, respectively [11]. The transmission power employed by the IEEE 802.11 nodes is typically two orders of magnitude larger than the sensornodes. It is known that such high power signals affect sensornode receivers by producing erasures scattered across a frame, significant enough to corrupt the reception [12]. Erasure codes allow recovery of corrupted frames while keeping the required transmission power in sensornodes low. The commodity IEEE 802.11 equipment is also affected by certain patterns of weak and narrow-band interference produced by sensornode transmissions [13]. Therefore, usage of erasure codes in the sensornodes, which allows to keep the transmission power low, improves coexistence, also benefiting the IEEE 802.11-based networks.

### III. PACKET SIZE OPTIMISATION

Various studies have shown that packet size has significant influence on packet reception rate [14], [15], [16]. Shorter packets are less likely to experience collisions (consequently reducing retransmissions), however, shorter packets also imply higher overheads, e.g., due to packet headers.

#### A. Short vs. Large Packets

The PRR comparison of ACK and data frames obtained from over  $1.20 \times 10^5$  packet transmissions, shown in Figure 1, illustrates a clearly increasing gap among the curves, as  $CQ$  diminishes. This gap stems from the ACK and data frame duration, i.e.,  $352 \mu$ s and  $4.256$  ms, respectively. It confirms that on an average, larger data frames undergo more frequent collisions. Observe the ordinates represent the median of PRR values corresponding to a  $CQ$  interval. This  $CQ$  quantisation is responsible for the 10% packet losses observed for  $CQ = 0.95$ , centred in the interval  $]0.9, 1.0]$ . We choose  $CQ$  sampling time of 50 ms corresponding to  $n = 2170$  samples,  $\beta = 0.3$ ,  $\tau = 5$  ms and  $E_{THR} = -65$  dBm. This value of  $E_{THR}$  produces a balanced distribution of  $CQ$  values across our trace set. We maintain these parameter values for all experiments, with the exception of  $\tau$ .

Due to the trade-offs mentioned earlier, it is expected that for a given interference level, a certain packet size maximizes the throughput and minimizes the total energy-per-useful-bit. To

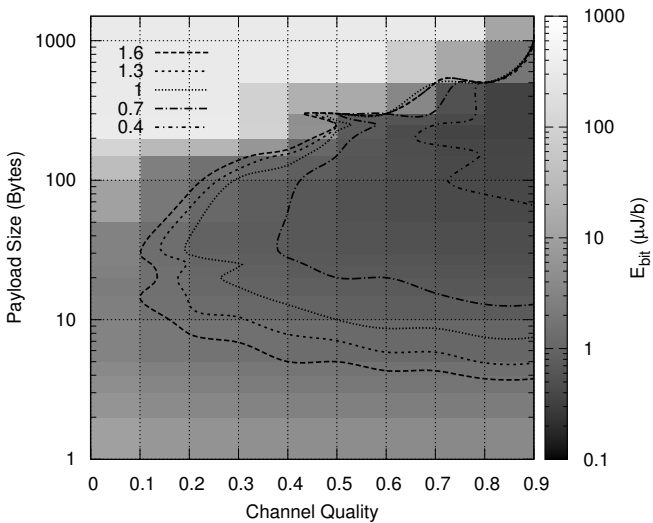


Fig. 2: Effects of packet size on energy-per-useful-bit  $E_{bit}$ , defined in Eq. 2. Outside the isogram the energy grows abruptly, specially on the upper side due to the higher number of collisions. The contour lines converge for large packet sizes and good channel qualities, i.e., in the upper right corner. As the channel quality gets close to 1 (i.e. perfectly idle channel), the optimal packet size diverges.

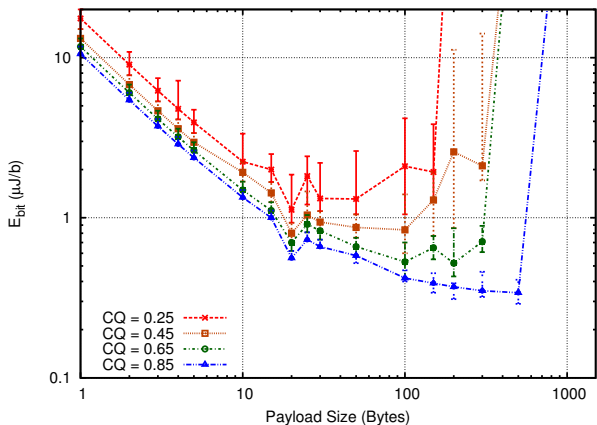


Fig. 3: Energy-per-useful-bit collected from over  $2.40 \times 10^5$  packets (ARQ only). Large packets provide more energy efficiency up to certain critical sizes depending on CQ values, above which the collision probability grows drastically and leads to very high values for  $E_{bit}$ .

investigate this, we conducted off-line experiments to compute the utility metrics introduced in Section §II-B.

### B. Payload Size Experiment

The IEEE 802.15.4 data frame contains a 6-byte PHY header and a 23-byte MAC header that includes an address field,

Packet Payload	NoP
$\leq 300$ bytes	7
500 bytes	5
1000 bytes	3
1500 bytes	2

TABLE II: Payload sizes and number of packets used per trace

followed by a payload of up to 102 bytes, and a 2-byte frame control sequence in the trailer [10]. Together, these headers account for around 25% of the maximum specified packet size. At a data rate of 250 kbps and 4 bits per symbol, as is commonly used in the IEEE 802.15.4-compliant radios operating in the 2.4 GHz band, each byte takes  $32 \mu\text{s}$  in the air. Thus, the PHY layer header lasts  $192 \mu\text{s}$  and a MAC header lasts from 224 to  $736 \mu\text{s}$ , depending on the address format. After the payload, the trailer lasts  $64 \mu\text{s}$ . In this experiment, we used a header duration of  $1024 \mu\text{s}$ , in order to analyse implications for 6LowPANs. This extended header accounts for 22 bytes of 802.15.4 PHY-MAC, including 64-byte addresses, and 10 bytes of compressed 6LowPAN header.

In this study, we explore our objective functions for packets with payloads in the range 1 to 1500 bytes, with varying channel quality quantified by CQ. Table II lists the payload sizes and the corresponding number of packets used per trace. In order to avoid fragmentation of packets whose size is larger than 127 bytes, the IEEE 802.15.4 standard requires increasing the 7-bit PHY frame length field by another 4 bits.

When actual data is transmitted over the channel, often an error control technique such as Automatic Repeat reQuest (ARQ), manages retransmissions of corrupted packets. In these off-line experiments, PRR accounts for the cost of retransmissions of packets with any single symbol altered due to interference. We refer to them as ARQ only to distinguish from those in which error correction is combined with ARQ.

### C. Experiment Results

Using the measurement data described in the previous section, we computed the PRR by checking whether collisions can occur due to the interference level exceeding the SINR threshold during a packet transmission. The outcome for same packet size, over traces whose CQ values fall within the same bin (bin-width = 0.1), are aggregated to compute the corresponding PRR value. This PRR value is then used in Equations 2 and 3. Packets are scheduled with a fixed interval,  $IPI = 7$  ms. We compute CQ over a trace segment of 50 ms and then run a PRR check over the entire trace.

Figure 2 shows that very small payloads lead to high  $E_{bit}$ . For highly interfered channels ( $0.3 < CQ < 0.6$ ), we find that there is a range of payload lengths from 20 to 100 bytes that provide low energy costs,  $1 \mu\text{J}/\text{bit}$  or less. The figure also shows that for congested channels, the energy required per useful bit for large packets is prohibitively high. We also find that the throughput is inversely correlated with the energy cost.

Payload sizes for the minimisation of  $E_{bit}$  are shown in Figure 3. A payload of around 100 bytes leads to good performance for all CQ values, which implies that a payload of this size is a good choice when no packet size adaptation is performed. This plot illustrates the energy improvements achievable by tuning the packet size for  $CQ \geq 0.6$ . However, the large inter-quartile ranges (IQR) for  $CQ \leq 0.6$

indicate large energy cost uncertainties, thereby limiting the effectiveness of packet size tuning. Thus, delay performance and effectiveness of retransmission schemes, when packet size adaptation is used, should be evaluated online.

When the channel quality is high ( $CQ \geq 0.85$ ), larger packets imply higher energy-efficiency and higher throughput. We encounter up to 20% increase in energy-efficiency and 240% gain in throughput for payload sizes up to 500 bytes compared to 100-byte payloads.

Vuran and Akyildiz proposed a packetARQ only size optimization framework for a multi-hop scenario and found energy optimal packet sizes up-to  $2 \times 10^4$  bytes, under SNR of 15 dB [16]. However, this experiment shows that in a low data-rate low-power PHY layer, up-to 500-byte payloads can be accommodated with cost benefits. These larger packets greatly increase throughput and by dynamically adjusting the packet size to the channel condition, energy-efficiency is maintained.

#### D. Implications for 6LoWPAN

These results are particularly relevant for 6LoWPAN networks. IPv6 requires the maximum transmission unit (MTU) to be at least 1280 bytes. In contrast, IEEE 802.15.4's standard maximum packet size is 127 octets. In the worst case the maximum size available for transmitting IP packets over an IEEE 802.15.4 frame is 81 octets. The IPv6 header is 40 octets long (without optional headers), which leaves only 41 octets for upper-layer protocols.

In order to cope with this constraint, RFC 4944 [17] proposes LoWPAN encapsulated IPv6 datagrams and header compression, which requires fragmentation and reassembly. However, increasing the IEEE 802.15.4 maximum packet size reduces header overhead, enhances link performance and boosts energy-efficiency. We have seen that it is beneficial in low interference scenarios. In the next section, we will discuss the use of erasure codes to enable large payload transmissions also in high interference scenarios. For an introduction to the design challenges related to 6LoWPAN and 802.15.4, the reader is referred to RFC 4919 [18] and RFC 4964 [17].

### IV. ERROR CORRECTION OPTIMISATION

Erasures codes are commonly used in storage and communication systems as an alternative and also as a complement to data redundancy and packet retransmissions. Proper use of erasure codes provides greater efficiency and fine-tunable levels of error protection, but at the cost of greater complexity.

In communication systems, error correcting codes are used as a Forward Error Correction (FEC) technique. Provided the receiver demodulator maintains synchronization, erasure codes can help recover packets despite collisions. In the presence of short duration interfering signals, as we show below, a small level of erasure code redundancy can lead to sizeable gains in terms of energy efficiency and performance.

We explore generic erasure codes and do not account for the computation cost of any particular realization of the coding

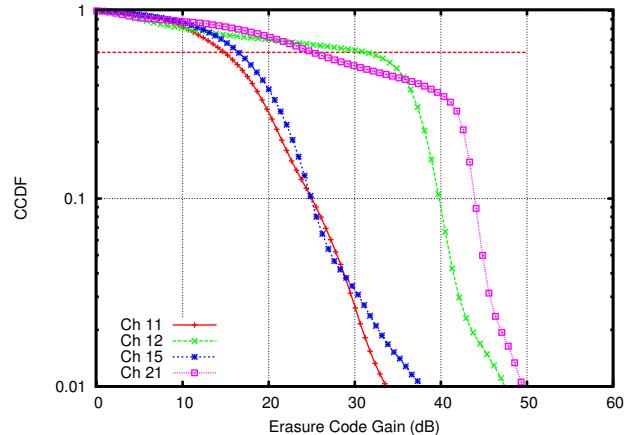


Fig. 4: Effective SINR gain due to erasure codes.

and decoding modules. Instead, our energy estimations are centred on radio chip power consumption and account for the consumption in both sender and receiver nodes. This is a reasonable approximation for next generation sensor networks platforms [2], [3], [4].

#### A. Equivalent SINR Gain

In order to understand the impact that FEC can have in the design of low-power wireless protocols, we investigate the equivalent SINR gain on the measurement data set discussed in Section §II-C. We compute the equivalent SINR gains as follows. With respect to a sliding window whose size corresponds to a fixed packet transmission duration, we compute: (a) the maximum level that the interference signal reaches inside the window and (b) we compute the minimum possible signal level (according to the SINR) at which the total length of erasures do not exceed the maximum correcting capacity of the erasure code being considered. The difference between these two signal values gives the equivalent SINR gain.

For each channel, the number of data points obtained by the sliding window samples is over  $9.70 \times 10^6$ , shown in Figure 4. The figure displays the Complementary Cumulative Distribution Function (CCDF) curves for four IEEE 802.15.4 channels, computed for a code capable of correcting 10% of the frame length. The values on the Y-axis represent the probability that the signal remains above a given power level, represented on the X-axis. Curves for all remaining channels fall in between the ones shown in the figure and are omitted for clarity. As the figure shows, an erasure code capable of recovering 10% of the packet payload provides an equivalent SINR gain of 25 dB with probability greater than 0.6 for a heavily interfered channel, like channels 12 and 21. There is also a significant gain of over 15 dB at the same probability for channels 11 and 15 which are much less interfered.

Observe the curves in Figure 4 corresponding to the IEEE 802.15.4 channels 11 and 21 have a prominently distant downswing point in the x-axis (10 and 40 dB, respectively),

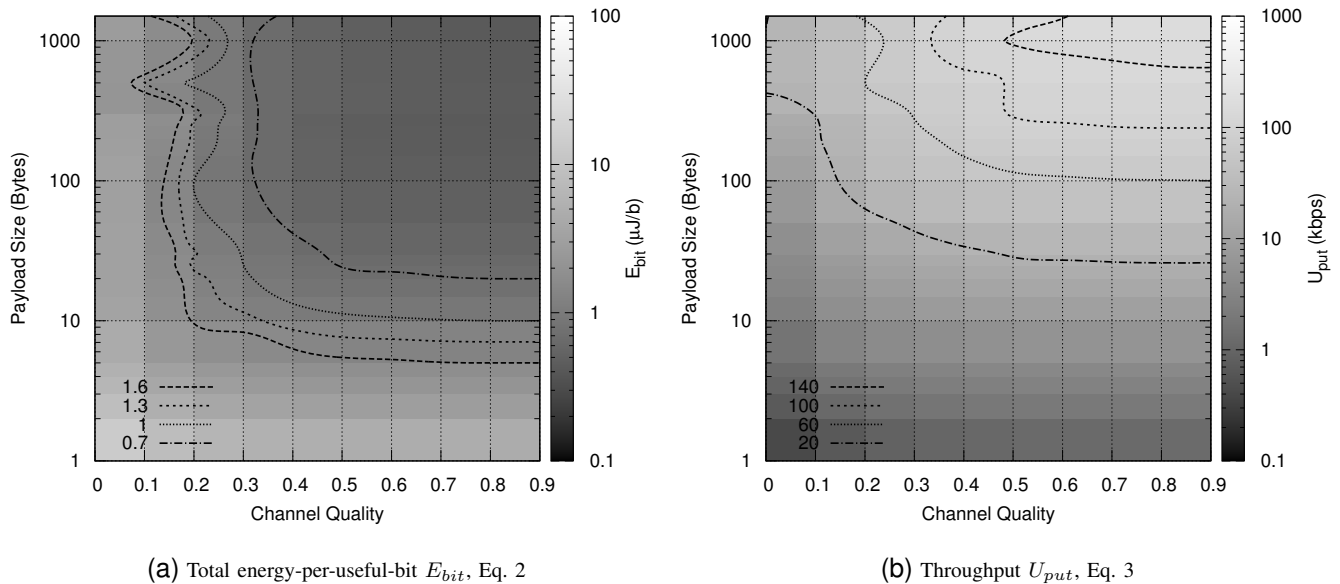


Fig. 5: Utility metrics with error correction ( $r = 0.8$ )

indicating that nodes in these channels are exposed to significantly different levels of interference from the IEEE 802.11 networks. Highly frequent spiky interfering signals shift the curves further to the right, corresponding to a larger power gain due to the erasure code. At small gain values, all curves exhibit similar slopes. In the absence of interfering signals, the code provides gains owing to the presence of noise. Therefore, all CCDF curves are similar for low gain values.

The CCDF curves are also very robust with respect to the size of the *sliding window*. Our experiments consistently reveal no difference between curves computed for intervals between 3 and 60 ms, when at least 10% payload is recoverable.

### B. Erasure Codes

Consider an optimal erasure code  $(n, k, t)$ , where  $n$  represents the length of the codewords,  $k$  the information bits to be mapped into the codewords, and  $t$  is the code correcting capacity. This code is capable to recovering the original message out of any  $k$  of the  $n$  codeword symbols. The worst case recoverable erasure of the optimal code is determined by the *Reiger bound* [19] and is given by  $t = 0.5(n-k)$ . Moreover, the code-rate  $r = \frac{k}{n}$  indicates the level of communication overhead the code introduces. We will further refer to this optimal erasure code as  $EC[r]$ . For a formal introduction to Erasure Codes (also called Burst-Error-Correcting Codes) please refer to [20, Ch. 20].

In the following study we use an erasure code  $EC[r]$  to partially encode frames and conduct a similar study to the one described in Section §III-C. In this case, the interference level may exceed the signal level leading to the SINR fall below the threshold during a frame reception. We mark the symbols erased whenever the SINR falls below the threshold. If the

amount of erased symbols remains below the level that the code can correct, the frame counts as successfully received.

PHY and MAC headers are typically added by dedicated hardware in the radio, after the transmission buffer is filled up with the rest of the frame. The checksum is computed prior to the inclusion of these headers, which leaves this part of the frame without error correction protection. First we consider this common scenario where PHY and MAC headers are not protected by a checksum and later on we consider the case for protecting the entire packet when the level of interference is extremely high.

Figure 5 shows the behaviour of utility metrics using a code  $EC[r = 0.8]$ . Similar to the previous section, packet sizes below 10 bytes lead to high energy cost and low throughput, regardless of the channel condition. However, a new result is that packet sizes up-to 1500 bytes lead to higher energy-efficiency. Energy values are below  $0.7 \mu\text{J}/\text{bit}$  and the surface is now flat for a wide range of packet sizes and channel conditions ( $CQ \geq 0.4$  and payloads  $\geq 30$  bytes) as shown in Figure 5a. The throughput surface in Figure 5b also shows significant improvements, as large packets provide nearly the maximum attainable throughput for low to moderate interference scenarios.

The impact of erasure codes is even more visible by comparing Figures 3 and 6. Despite that heavy interference still doubles the energy cost, the overall energy-per-useful-bit remains nearly flat even for low channel qualities. In the experiments discussed earlier in Section §III-C, packets contain vulnerable frames with headers lasting  $1024 \mu\text{s}$  followed by the payload. The header contains 22 bytes of 802.15.4 PHY-MAC (64-byte addresses) and 10 bytes of compressed 6LoWPAN header. In contrast, in these FEC experiments, the vulnerable

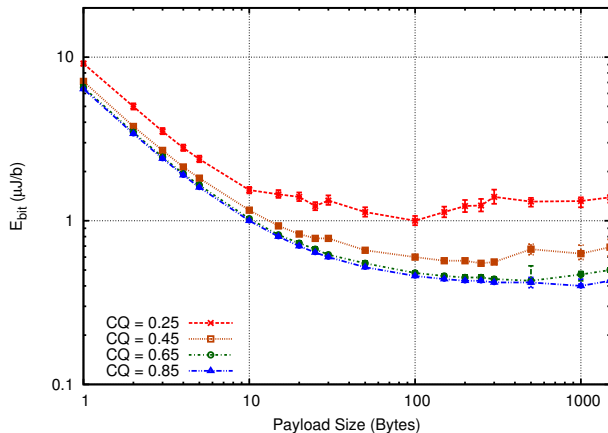


Fig. 6: Energy optimization with error correction  $EC[r = 0.8]$ : Payload size vs. energy-per-useful-bit.

frame section lasts  $480 \mu s$  and the rest is protected by the code. As a consequence there is lower probability of frame errors due to collisions. Comparing the origin of the curves (negligible payload size) in Figures 3 and 6, shorter vulnerable headers cut the energy-per-useful-bit by nearly 50%.

Furthermore, the large IQR bars for  $CQ \leq 0.6$  observed in Figure 3 are shrunk by the erasure code. The erasure code introduces tolerance for changes in the interference situation between the instant  $CQ$  is computed and when the frame arrives. In other words, in the experiments in Section §III-C, small changes in interfering energy spikes may create collisions that change the PRR values for the same  $CQ$  values. With the erasure code, it requires a much larger change in the interference scenario to make an equivalent difference in the PRR.

In Figure 7, we present a comparison of optimal payload sizes and the maximum throughput obtained using erasure codes and those obtained using ARQ (as in Section §III-C). The payload size and the throughput increase by almost 5 times in high interference scenarios using erasure codes. The improvements continue to hold for the wide range of  $CQ$ , except for very high quality channels. For perfectly idle channels, the code introduces an unnecessary overhead.

We explore the effects of various code-rates on the utility metrics. We found that for  $r \leq 0.6$  there is no significant improvement. The added correction capacity provided by  $EC[r = 0.6]$  is useless without also adding protection to all headers. We discuss this in more detail in the next section.

This experiment shows that erasure codes further extend optimal packet sizes up-to 1500-byte payloads. These large packets boost performance and energy-efficiency under heavy interference from Wi-Fi networks. These results agree with previous findings by Vuran and Akyildiz [16] and point toward sizeable cost benefits in extending the maximum packet size in the low-power low-datarate PHY. Furthermore, large packet sizes may not be a limitation for future sensor networks platforms [4].

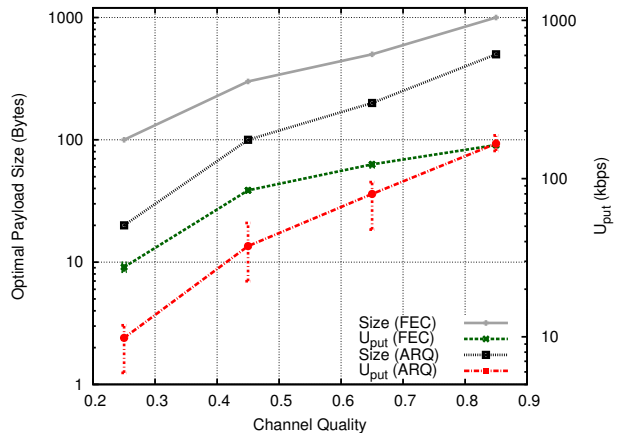


Fig. 7: Optimal payload sizes and the corresponding throughput for ARQ and  $EC[r = 0.8]$ .

### C. $CQ$ -based FEC Optimisation

We now discuss the use of the wireless channel quality metric ( $CQ$ ) to dynamically adapt the payload size and FEC overheads.

We compared the performance gains of erasure codes  $EC[r = 0.6]$  and  $EC[r = 0.8]$  for low channel qualities, and found little or no difference. Moreover, the number of unrecoverable packets was independent of their sizes. This was due to the fact that the errors were located in the unprotected headers. Thus, to investigate the effectiveness of  $EC[r = 0.6]$ , we left only the PHY header vulnerable, which is 6-byte long and hence lasts  $192 \mu s$ . In this case, we found performance improvements for  $CQ \leq 0.3$ .

We studied these two codes,  $EC[r = 0.6]$  and  $EC[r = 0.8]$ , and ARQ on frames containing 100-byte payloads. The result is shown in Figure 8. In the figure, we can identify three regions based on the behaviour of the code. Each region corresponds to a range of  $CQ$  values, which we simply refer to as *low*, *medium* and *high* channel qualities. In each of these regions there is one code-rate that provides the optimum results for both utility metrics, energy as well as throughput. These new results indicate that there are between 20 to 60% improvements in both energy-per-bit and throughput, over the entire  $CQ$  range. Moreover, we find that both utility metrics favour larger payloads.

From these evaluations, we make the following observations: (a) optimal payload sizes increase with  $CQ$ , for all code-rates, (b) lower code-rates lead to larger optimal payload sizes, (c) for each channel quality range (*low*, *medium* and *high*), there is a code-rate that improves the utility metrics regardless of the payload sizes, and for a given  $CQ$  larger payloads perform better on the utility metrics. This can be seen in Figures 7 and 8.

Based on these experimental results, we propose the following algorithm, RR-ADAPT, to dynamically adapt radio resources in a receiver initiated MAC protocol, e.g., A-MAC [21]. RR-ADAPT determines the optimal settings for data transfer on channels affected with interference including CTI. This

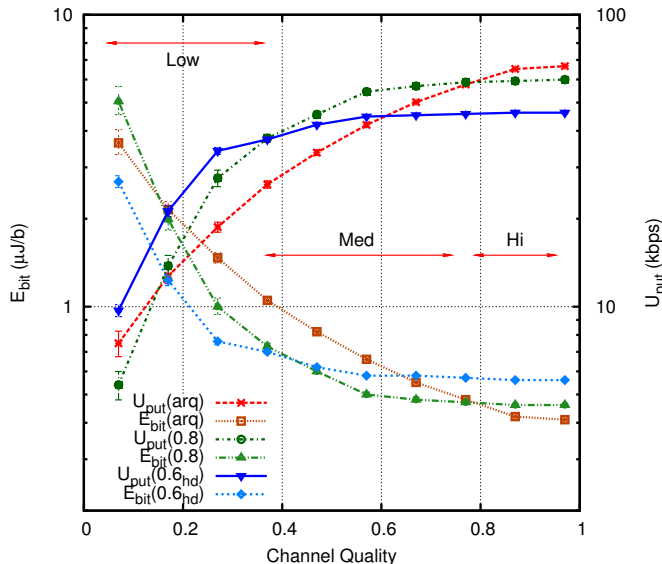


Fig. 8: Optimal error control for three channel quality regions: *Low CQ-FEC(0.6)*, *Medium CQ-FEC(0.8)* and *High CQ-ARQ*.

algorithm takes as inputs the energy level of the frame’s signal reaching the receiver ( $E_{THR}$ ) and the data volume to be transferred from the sender. It then provides the optimal payload sizes and code-rate as follows: it computes  $CQ$  based on  $E_{THR}$  and finds the optimal code-rate from off-line results, such as the one in Figure 8. It then finds the optimal payload based on  $CQ$  and  $r$ , from the curves in Figure 7. The receiver computes the  $CQ$ , and then inserts the  $CQ$  value in the MAC probe, sent periodically at the end of each sleep cycle. The sender prepares packets accordingly before transmitting. To the best of our knowledge, there are no IEEE 802.15.4 transceivers as yet that can handle very large ( $\sim 1000$  bytes) packets. Therefore, we leave validating these ideas in online experiments as a future work.

## V. RELATED WORK

Vuran and Akyildiz present a cross-layer solution for packet size optimization considering multi-hop routing and error control techniques [16]. They conclude that the increase in payload length decreases the MAC failure rate. In contrast, we study a point-to-point link scenario considering the overhead of packet headers and collisions due to external interference using real-world measurement data.

Huang et al. study self-similarity of Wi-Fi *white spaces*, propose a Pareto model characterize them and a control mechanism to fragment IEEE 802.15.4 frames [22]. We share the goal of adapting to the channel condition but computing  $CQ$  solely relies on channel energy detection by the receiver and does not require any packet transmissions. Therefore, it scales with node density and channel usage. Also, when the overhead of 6LoWPAN headers is considered, fragmented packets below 127 bytes are not energy efficient as we have presented in this

paper.

Hermans et al. [23] classify the interference source based on corrupted packets in order to use appropriate mitigating strategies. Boers et al. [24] study signal strength traces for high-level classification of interference patterns. Instead, our  $CQ$  metric ranks the channel, based on consecutive vacancies, and is inherently agnostic to the interference source.

Hong et al. present mote-in-the-loop, an approach to optimize communication strategies such as packet size and retransmission schemes [25]. They superimpose replayed interference traces on normal communication to study the effect of interference and optimize communication strategies accordingly. Their off-line approach is orthogonal to our online approach. However, they can be combined by using mote-in-the-loop to determine the initial configuration and our  $CQ$ -based method to fine-tune the parameters online.

Recently, we have described the preliminary design of the  $CQ$  metric [6]. Compared to this early work, the main contribution of this paper is the application of the  $CQ$  metric for resource adaptations in energy-constrained low-power wireless networks. Here we address the issue of managing uncontrollable CTI in order to enable co-existence with other networks.

## VI. CONCLUSION

We addressed the issue of co-existence of low-power wireless networks in the presence of cross-technology interference from uncontrollable sources, which may operate at high power levels. We presented an online metric,  $CQ$ , to evaluate wireless channel quality. Using this metric, we studied dynamic packet size adaptation and the application of erasure codes for optimizing reliability, energy consumption and throughput. Based on measurement data collected from a building containing several Wi-Fi networks, we showed that for moderate and low interference levels, increasing the packet size to a few hundred bytes, i.e. beyond the limit specified in the IEEE 802.15.4 standard, can lead to significant improvements in network performance. We also showed that erasure codes drastically improve energy-efficiency and throughput of low-power wireless links, remaining cost-effective for large payload sizes, e.g., 1000–1500 bytes.

## ACKNOWLEDGEMENTS

This work was partially supported by National Funds through FCT (Portuguese Foundation for Science and Technology) and by ERDF (European Regional Development Fund) through COMPETE (Operational Programme ‘Thematic Factors of Competitiveness’), within MASQOTS project, ref. FCOMP-01-0124-FEDER-014922; also by SSF (Swedish Foundation for Strategic Research), FCT and ESF (European Social Fund) through POPH (Portuguese Human Potential Operational Program), under PhD grant SFRH/BD/62198/2009.

## REFERENCES

- [1] C. A. Boano, T. Voigt, N. Tsiftes, L. Mottola, K. Römer, and M. Zúñiga, “Making Sensornet MAC Protocols Robust Against Interference,” in *Proc. of the 7th EWSN*, Coimbra, Portugal, Feb. 2010, pp. 272–288.

- [2] R. Jurdak, K. Klues, B. Kusy, C. Richter, K. Langendoen, and M. Brünig, "Opal: A Multiradio Platform for High Throughput Wireless Sensor Networks." *Embedded Systems Letters*, pp. 121–124, 2011.
- [3] J. Ko, K. Klues, C. Richter, W. Hofer, B. Kusy, M. Brünig, T. Schmid, Q. Wang, P. Dutta, and A. Terzis, "Low Power or High Performance? A Tradeoff Whose Time Has Come (and Nearly Gone)," in *EWSN*, 2012.
- [4] E. Micro, "Energy Friendly Radios: EFR4D2090 Datasheet," <http://www.energymicro.com/draco>, Jun. 2012, Confidential/Preliminary, Provided as Registered Copy.
- [5] M. Goyal, S. Prakash, W. Xie, Y. Bashir, H. Hosseini, and A. Durrresi, "Evaluating the Impact of Signal to Noise Ratio on IEEE 802.15.4 PHY-Level Packet Loss Rate," in *Proc. of the 13th NBIS*, Los Alamitos, CA, USA, 2010, pp. 279–284.
- [6] C. Noda, S. Prabh, M. Alves, C. A. Boano, and T. Voigt, "Quantifying the Channel Quality for Interference-aware Wireless Sensor Networks," *ACM SIGBED Rev.*, vol. 8, pp. 43–48, Dec. 2011.
- [7] C. Noda, S. Prabh, M. Alves, T. Voigt, and C. A. Boano, "CRAWDAD data set cister/rssi (v. 2012-05-17)," Downloaded from <http://crawdada.cs.dartmouth.edu/cister/rssi>, May 2012.
- [8] J. Ammer and J. Rabacy, "The energy-per-useful-bit metric for evaluating and optimizing sensor network physical layers," in *Proc. of the 3rd Annual IEEE SECON*, vol. 2, sept. 2006.
- [9] *Smart RF CC2420 datasheet - 2.4 GHz IEEE 802.15.4 / ZigBee-Ready RF Transceiver (Rev. B)*, Swrs041b ed., TI (Chipcon), Mar. 2007, <http://focus.ti.com/lit/ds/symlink/cc2420.pdf> - Last visited April 2013.
- [10] *Wireless Medium Access Control (MAC) and Physical Layer (PHY) Specifications for Low-Rate Wireless Personal Area Networks (WPANs)*, Rev. 802.15.4-2006 ed., IEEE 802.15.4 Working Group, Sep. 2006.
- [11] *Wireless LAN MAC and PHY Specifications*, IEEE Std 802.11-2007 ed., IEEE 802.11 Working Group, Jun. 2007.
- [12] C. Liang, B. Priyantha, J. Liu, and A. Terzis, "Surviving Wi-Fi Interf. in low power ZigBee Networks," in *Proc. of the 8th ACM SenSys*, Zurich, Switzerland, 2010.
- [13] R. Gummadi, D. Wetherall, B. Greenstein, and S. Seshan, "Understanding and mitigating the impact of RF interference on 802.11 networks," in *Proc. of the ACM SIGCOMM*. Kyoto, Japan: ACM, 2007.
- [14] Y. Sankarasubramaniam, I. F. Akyildiz, and S. W. McLaughlin, "Energy Efficiency Based Packet Size Optimization in Wireless Sensor Networks," in *Proc. of the 1st Workshop on Sensor Network Protocols and Applications*, Jun. 2003.
- [15] C. A. Boano, T. Voigt, C. Noda, K. Römer, and M. Zúñiga, "JamLab: Augmenting Sensornet Testbeds with Realistic and Controlled Interference Generation," in *Proc. of the 10th IPSN*, Chicago, USA, Apr. 2011, pp. 175–186.
- [16] M. C. Vuran and I. F. Akyildiz, "Cross-layer Packet Size Optimization for Wireless Terrestrial, Underwater, and Underground Sensor Networks," in *27th IEEE INFOCOM*, Phoenix, AZ, USA, 2008.
- [17] G. Montenegro, N. Kushalnagar, J. Hui, and D. Culler, "Transmission of IPv6 Packets over IEEE 802.15.4 Networks," RFC 4944 (Proposed Standard), Internet Engineering Task Force, Sep. 2007, updated by RFC 6282. [Online]. Available: <http://www.ietf.org/rfc/rfc4944.txt>
- [18] N. Kushalnagar, G. Montenegro, and C. Schumacher, "IPv6 over Low-Power Wireless Personal Area Networks (6LoWPANs): Overview, Assumptions, Problem Statement, and Goals," RFC 4919 (Informational), Internet Engineering Task Force, Aug. 2007. [Online]. Available: <http://www.ietf.org/rfc/rfc4919.txt>
- [19] S. Reiger, "Codes for the Correction of 'Clustered' Errors," *Information Theory, IRE Transactions on*, vol. 6, no. 1, pp. 16–21, march 1960.
- [20] S. Lin and D. J. Costello, *Error Control Coding, Second Edition*. Upper Saddle River, NJ, USA: Prentice-Hall, Inc., 2004.
- [21] P. Dutta, S. Dawson-Haggerty, Y. Chen, C.-J. M. Liang, and A. Terzis, "Design and evaluation of a versatile and efficient receiver-initiated link layer for low-power wireless," in *Proc. of the 8th ACM SenSys*, Zurich, Switzerland, 2010.
- [22] J. Huang, G. Xing, G. Zhou, and R. Zhou, "Beyond co-existence: Exploiting WiFi white space for Zigbee performance assurance," in *Proc. of the The 18th IEEE ICNP*, Washington, DC, USA, 2010.
- [23] F. Hermans, O. Rensfelt, T. Voigt, E. Ngai, L. Larzon, and P. Gunningberg, "SoNIC: Classifying Interference in 802.15.4 Sensor Networks," in *Proc. of the 12th ACM IPSN*, Philadelphia, USA, Apr. 2013, pp. 55–66.
- [24] N. M. Boers, I. Nikolaidis, and P. Gburzynski, "Sampling and Classifying Interference Patterns in a Wireless Sensor Network," *ACM Trans. Sen. Netw.*, vol. 9, no. 1, pp. 2:1–2:19, Nov. 2012.
- [25] M. Hong, E. Björnemo, and T. Voigt, "Exploring sensor network communication strategies with the mote-in-the-loop approach," in *Proc. of the 14th WPMC*, Oct. 2011.